Experimental Verification of the Error-Rate Performance of Two Types of Regenerative Repeaters for Differentially Coherent Phase-Shift-Keyed Signals

By W. M. HUBBARD and G. D. MANDEVILLE

(Manuscript received February 9, 1967)

High-speed digital repeaters are being considered in the Bell System and elsewhere for both long- and short-haul communication systems. This paper describes two devices which were built to serve as prototypes of the IF portion of a millimeter guided-wave communication system but which might serve equally well as the IF portion of the repeaters for an optical communication system or for microwave radio systems. These two prototypes, designed for a differentially coherent phase-shift-keyed (DCPSK) signal, have been built and operated at a bit rate of 160 Mb/s using an 11.2-GHz IF signal. Both models operated with error rates very close to those predicted theoretically. One of the models seems to be particularly suitable for such systems; it consists of comparatively simple circuitry, and its operation is within 0.5 dB of the theoretical ideal behavior for a DCPSK system.

I. INTRODUCTION

High-speed long-haul communication by means of millimeter waves transmitted in the circular electric mode through a multimode circular waveguide was described by S. E. Miller[1] in 1954, and subsequently considered in some detail by Rowe and Warters.[2] This paper describes two experimental models of the IF portion of a repeater for such a system and compares their performance with theoretical predictions of error rate. These models could serve equally well as IF sections of repeaters for optical communication systems or microwave radio systems.

No attempt is made in these models to equalize the delay distortion of the medium, and no allowance is made for degradation from up converters, down converters, and millimeter-wave circuitry.

Both experimental model repeaters operated at a bit rate of 160 Mb/s and used an IF of 11.2 GHz. The bit rate and the IF were arbitrary choices made for convenience. In an actual system, a somewhat lower IF would be chosen to facilitate building solid-state amplifiers and a somewhat higher bit rate would probably be desirable. Since these model repeaters were to serve as prototypes for an even higher bit rate repeater, no components were used which did not seem capable of being modified to operate up to about twice this bit rate.

Section II discusses briefly the two particular choices of modulation scheme which were used, and describes some of the features common to both models. Section III describes the so-called AM-DCPSK repeater and Section IV the FM-DCPSK one.

These models demonstrated that a repeater which performs with error rates quite close to those predicted theoretically can be built.

II. DIFFERENCES AND SIMILARITIES OF THE TWO MODELS

The final version of a millimeter-wave repeater would almost certainly be an all solid-state system. This requirement imposes a limitation on the maximum power available, especially at millimeter-wave frequencies. Because of this power limitation, which generally manifests itself as a limitation on peak power, it is necessary to use a modulation scheme which affords good noise immunity. Optimum noise immunity (in a binary system) is obtained when the two signal states are anticorrelated.[3] This corresponds to coherent phase modulation where the two signals have identical envelopes (consistent with the power limitations) and differ in phase by π radians. Such a system operates by sending pulses with phase either 0 or π relative to some standard reference phase. With a system of this type, it is necessary to provide this standard phase at each repeater in order that regeneration may be performed. An alternative approach is differentially-coherent phase-shift-keying (DCPSK). In DCPSK, the phase of each pulse is used as the reference for determining the phase of the next following pulse. The information is, therefore, carried in the relative phase or, equivalently, it is carried in whether or not the phase changes between pulses. The penalty in noise immunity for using a DSPSK system instead of a coherent PSK system amounts to about 2 dB for error-rates of about 0.01 but decreases with increasing S/N. For signal-to-noise ratios which give error-rates of the order of 10^{-9} (the assumed acceptable error-rate for this experiment) the degradation in noise immunity is less than 0.5 dB. (See, for example,

Lawton.[4]) Since the system under consideration is to be operated with error rates of this order, the only form of modulation to be considered in this paper is DCPSK.

A block diagram of a typical repeater is shown in Fig. 1. The purpose of this figure is to show the overall layout of the repeater and to indicate where the IF portion of the repeater fits in. Figs. 2 and 3 are block diagrams of the two experimental model repeaters which this paper describes, along with the test equipment used in the experiments. The portions of these figures contained within the dotted lines are more detailed versions of the single block labeled "IF portion" in Fig. 1.

The two model repeaters used somewhat different modulation schemes to achieve the binary DCPSK. In binary DCPSK, the information is carried in the phase *change* of a signal between two sampling points. DCPSK signals can have several forms since the only requirement is that the phase must make either of two prescribed changes between each pair of adjacent sampling points. Two somewhat idealized classes of signals are considered below. These two classes represent limiting cases since any physically realizable signal would contain some of the properties of each. We designate these classes as AM-DCPSK and FM-DCPSK. The AM-DCPSK signals are created (at least conceptually) by generating a separate pulse for each time slot with one or the other of two phases. Each pulse is thought of as being generated independently of pulses in other time slots, but is not necessarily confined to a single time slot, i.e., intersymbol interference is allowed. As an example, such a signal might have the form

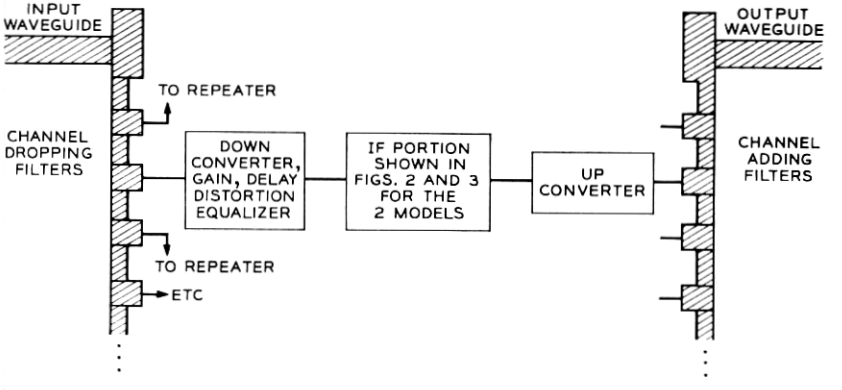

Fig. 1 — Block diagram of a complete repeater.

$$S(t) = \sum_{n=0}^{N} S_0(t - nT) \exp [j(\omega t + \alpha_n)], \tag{1}$$

where $S_0(t)$ is the pulse-shaping factor which is slowly varying compared with the exponential factor, and α_n is a chance variable which can take with equal probability either of two values which differ by π. The information is carried in whether $| \alpha_{n-1} - \alpha_n |$ equals 0 or π. In such a system, the amplitude is varied, but the carrier frequency of the individual pulses, $\omega/2\pi$, is a constant. If the pulses were nearly resolved, i.e., if

$$| S_0(t) | \ll S_0(0) \qquad \text{for} \qquad | t | \geqq T/2 \tag{2}$$

$S(t)$ would look like a pure AM signal as illustrated in Fig. 4(b).

The FM-DCPSK class is one in which the amplitude of the signal remains constant and the phase change (if any) between adjacent sampling times is effected by changing the carrier frequency. As an example, such a signal might have the form

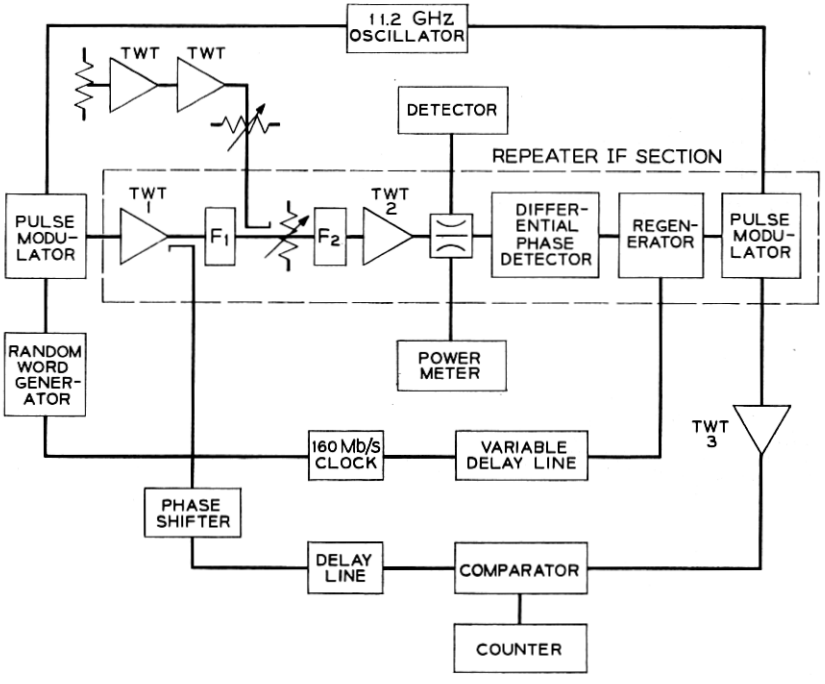

Fig. 2 — Block diagram of the AM-DCPSK model repeater.

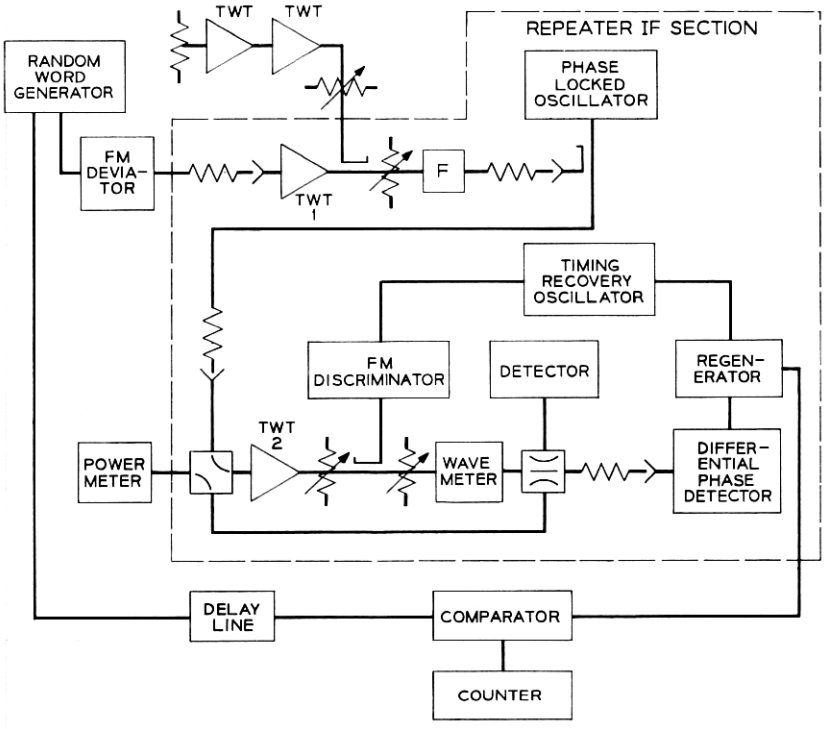

Fig. 3 — Block diagram of the FM-DCPSK model repeater.

$$S(t) = \exp j\left\{\omega_0 t + \int_0^t \omega(t')\, dt'\right\}, \quad \text{where} \quad \int_{(n-1)T}^{nT} \omega(t')\, dt' = \alpha_n \quad (3)$$

and α_n is as defined for the AM-DCPSK system. An example of such a signal is shown in Fig. 4(d).

The signals used in the repeater to be described in Section III were essentially the AM-DCPSK class, although, in practice, some frequency modulation of the tails of the pulses is inevitable. Signals used in the repeater described in Section IV were essentially of the FM-DCPSK class, although some amplitude modulation is inevitable due to the finite bandwidth of the devices used in the experiment.

The AM-DCPSK signal has the advantage that a comparatively complete theoretical analysis of error rate in the presence of intersymbol interference is available. The FM-DCPSK signal has two advantages, namely, that a phase-locked oscillator can be used to pro-

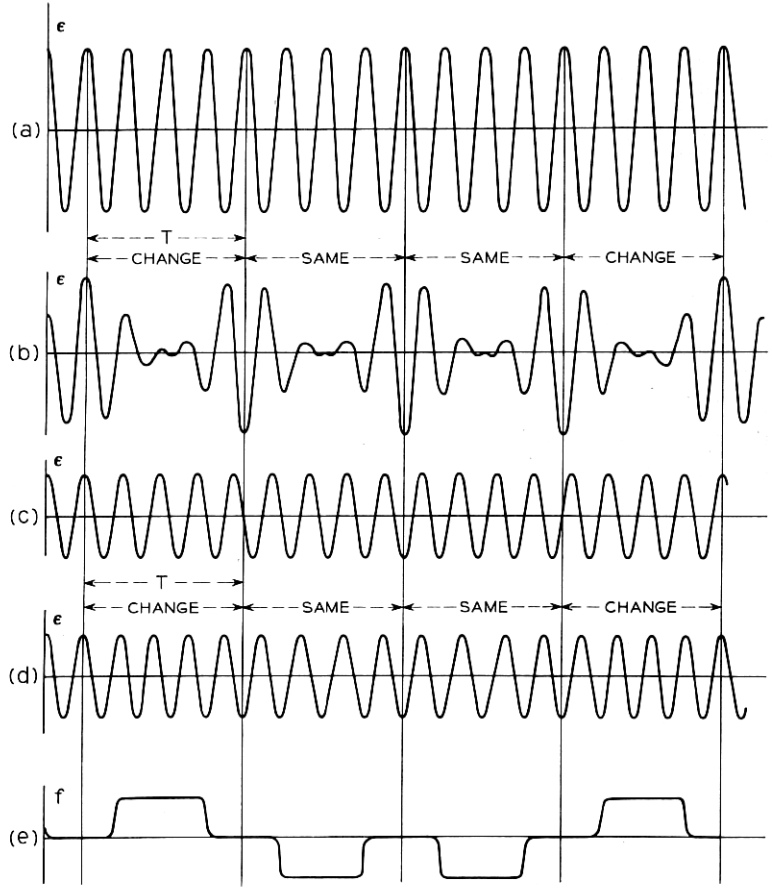

Fig. 4 — (a) unmodulated IF-carrier for AM-DCPSK; (b) idealized AM-DCPSK signal; (c) unmodulated IF-carrier for FM-DCPSK; (d) idealized FM-DCPSK signal carrying the same information as in (b); (e) frequency vs time for the signal in (d).

vide limiting and gain, and that it is comparatively easy to recover timing directly from the signal.

Certain features of the model repeaters shown in Figs. 2 and 3 are identical. Others are quite different. The components which are common to both models are described below. The others are described in Sections III and IV.

All of the traveling-wave tubes used are BTL experimental Model M1917.

2.1 *Random Word Generator*

The random word generator circuitry (for both experimental model repeaters) is identical to the baseband regenerator used with the AM-DCPSK model (to be described in Section III). Wideband random noise from three cascaded amplifiers is used for a random input signal to this "regenerator." The output is, therefore, a sequence of random positive and negative pulses occurring at the 160-megabit rate.

2.2 *Differential Phase Detector*

The differential phase detector ($D\varphi D$) is shown in Fig. 5. This device is used in both models as the $D\varphi D$ and, in addition, an adaptation of the device is used in the comparator for the AM-DCPSK model and another adaptation is used in the timing recovery circuit of the self-timed version of the FM-DCPSK model. The behavior of this device is discussed in the appendix of Ref. 5 for an FM-DCPSK signal. The behavior of the device with one time slot delay for an AM-DCPSK signal is quite straightforward and will be discussed briefly in Section III.

III. THE AM-DCPSK REPEATER

3.1 *General Description of the AM-DCPSK Repeater*

A block diagram of the AM-DCPSK Repeater is shown in Fig. 2. A random binary signal (at baseband) is provided by the random word generator at a bit rate of 160 Mb/s. This random "message" is then transferred onto the 11.2-GHz carrier by the first pulse modulator—

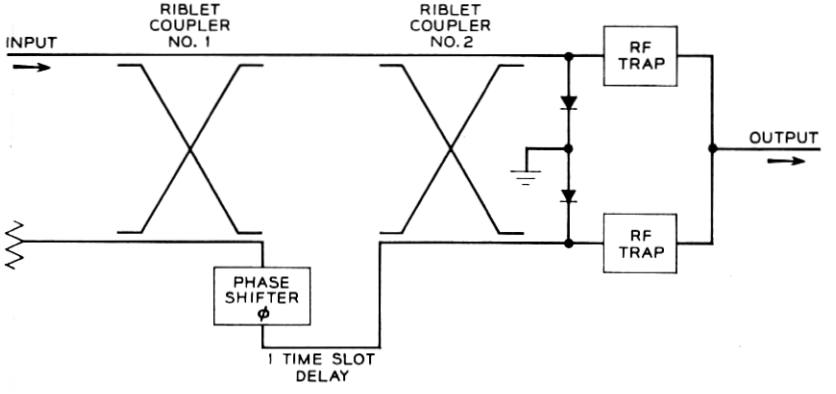

Fig. 5 — Differential phase detector ($D \varphi D$).

the two states now being the two phases 0 or π. The pulse signal is then amplified by TWT 1. Part of the signal (hereafter called the reference signal) is then tapped off in the directional coupler and stored in the delay line for later comparison with the regenerated signal. The remainder of the signal passes through filter F_1. Noise is added to the signal and the combined signal and noise are filtered by F_2 and amplified by TWT 2. The differential detector then processes this corrupted signal and the regenerator makes the decision as to whether a change or a same has occurred, regenerates a positive or negative pulse accordingly, translates back into differential binary and regenerates the translated signal into a form suitable for driving the second pulse modulator. This second pulse modulator (which derives its CW from the same source, a klystron, as the first pulse modulator) then provides a signal which carries the same message (except where errors are made) as the output of the first pulse modulator. This signal is amplified and combined with the reference signal in the comparator. The comparator then signals the counter when an error has been made.

3.1.1 *Differential Phase Detector for AM-DCPSK Pulses*

The AM-DCPSK signal is of the form given in (1). Straightforward analysis of Fig. 5 (assuming ideal square-law detectors) with the delay path equal to one bit interval shows the output of the $D\varphi D$ to be

$$\tfrac{1}{2}S_0^2(0)\cos(\alpha_n - \alpha_{n-1} - \varphi)$$

at the middle (the sampling time) of the nth time slot. For $\varphi = 0$, this signal is $+\tfrac{1}{2}S_0^2(t)$ when $\alpha_n = \alpha_{n-1}$ and is $-\tfrac{1}{2}S_0^2(t)$ when $\alpha_n = \alpha_{n-1} \pm \pi$. For $\varphi = \pi$ the opposite result obtains.

In the actual experiment, the signals are corrupted by both intersymbol interference and noise. The regenerator must make its decision on the basis of this corrupted signal and respond accordingly.

3.1.2 *Pulse Modulator*

The pulse modulators convert an 11.2-GHz CW signal into pulses having one of two possible phase states in accordance with the baseband signal pulse. Positive drive pulses produce an output of one phase and negative drive pulses produce an output shifted by 180 degrees.

The modulator consists of a Western Electric 2B hybrid junction with a matched pair of 1N78 diodes shunting the conjugate arms. One

arm contains a phase shifter in addition to the diodes. The device is shown schematically in Fig. 6.

The operation of the modulator depends upon the return loss of the diodes and the balance between them. They are dc biased to be matched so that very little power is reflected from them. Application of a baseband pulse to the diodes then produces reflected RF pulses in the conjugate arms. With the proper setting of the phase shifter they will add in the output circuit yielding an output pulse. When the drive pulse is of the opposite polarity, the reflected signals in the conjugate arms both differ by 180 degrees from the previous case. The resulting output pulse is then also shifted by 180 degrees.

In practice the phase shift from one state to the other is found to be 180 $\pm$ 5 degrees. The $\pm$5 degrees represents the limit of accuracy of the measurement. The modulator loss, (the ratio of CW power in to pulse power out) increases as the CW input drive is increased or as the baseband drive is decreased. Under the low-drive conditions used in this experiment this loss is of the order of 20 dB.

3.1.3 *Baseband Regenerator*

The baseband regenerator (Fig. 7) samples the polarity of the differential detector output at the center of the time slots and translates this information into an output train of equal amplitude positive and negative pulses which are converted into 0 or π RF phases in the pulse modulator. In the absence of errors, this pulse train has a one-to-one correspondence with the original signal.

The regenerator consists of three direct-coupled stages of tunnel-

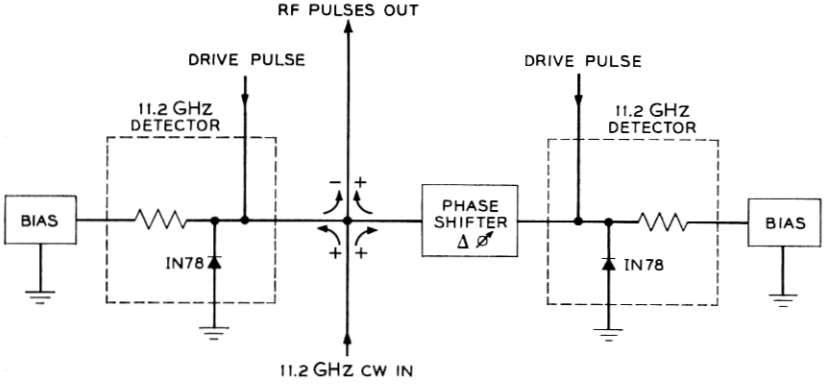

Fig. 6 — Pulse modulator schematic diagram.

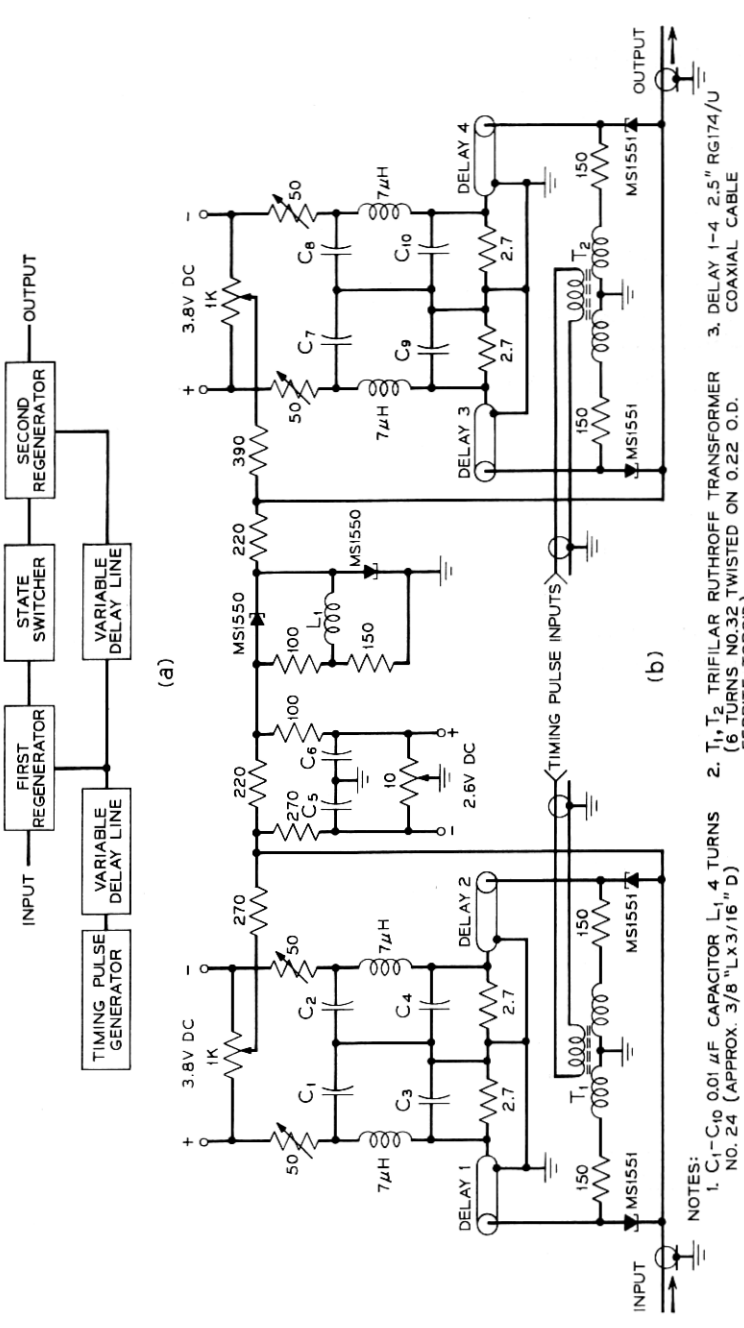

Fig. 7 — (a) Baseband regenerator; (b) baseband regenerator-schematic.

diode pairs. The first and third stages are a form of Goto-pair majority-logic circuit triggered at the 160-Mb/s rate by 1-nsec timing pulses. The middle stage is an adaptation of a well-known "flip-flop" circuit.

The input signal for the first stage is the output of the differential phase detector. (Some delay is provided in the coupling to minimize interference between the input signal and the pulses generated by the first stage.) The timing of the 160-Mb/s triggering pulses is adjusted so that they coincide with the centers of the time slots of the input signal. An output pulse is triggered in every time slot; its polarity is dependent upon the majority polarity of the input signal at the sampling time.

The second stage, the state-switcher, consists of two tunnel-diodes connected in series. Each time a positive pulse arrives the diodes exchange states. The diodes remain in their respective states so long as no positive pulse appears. The circuit time constant allows changes to be made as fast as the maximum requirement of the system—up to once every 6.25 nsec.

When the diodes exchange states the voltage at the junction of the two diodes changes between two discrete values relative to ground. This point is coupled to the junction of the third stage diode pair, and the timing of the third stage triggering pulse is adjusted so as to have decision times occur midway between any possible state changes.

The third stage, operating exactly as the first stage, then puts out pulses which are positive when the state switcher is in one state and negative when it is in the other state. These output pulses provide the drive for the RF pulse modulator described earlier.

3.1.4 *Comparator*

The function of the comparator is to compare the regenerated version of the corrupted signal with the uncorrupted reference signal and to indicate to the counter when an error has been made by the regenerator. Information in a DCPSK signal is carried not by the phase of an individual pulse but by the relative phase between adjacent pulses. The four possible situations are listed in Table I.
In the first two situations in Table I, an error was made; in the last two, no error was made.

As an example, the signal with phases

$$0\ 0\ \pi\ 0\ \pi\ \pi\ 0$$

is equally well represented, after regeneration, by itself or by its exact

TABLE I — POSSIBLE RELATIVE INFORMATION COMBINATIONS IN THE COMPARATOR

Relative phase between two reference pulses	Relative phase between two corresponding regenerated pulses
Change (π)	Same (0)
Same (0)	Change (π)
Same (0)	Same (0)
Change (π)	Change (π)

opposite, viz.,

$$\pi\ \pi\ 0\ \pi\ 0\ 0\ \pi.$$

We can refer to the case where the regenerator is reproducing the input exactly as the "G mode" and the case where it is reproducing the opposite of the input as the "U mode." (Such a distinction has meaning only where some absolute phase reference exists for the original and regenerated signals. This is the case in our experiment since both modulators are supplied from the same RF source; this is probably not the case in an actual system where the regenerated signal would not necessarily be transmitted at the same carrier frequency as the incoming signal.)

A little thought will convince the reader that the effect of an error by the regenerator is to cause the regenerated signal to change modes (U to G or G to U). In our example of the preceding paragraph, suppose that the change between the third and fourth symbols is (erroneously) interpreted by the regenerator (due to noise) to be a same. If the regenerator was originally functioning in the G mode, the result would be as shown

$$\text{Input}: \quad 0\ 0\ \pi\ 0\ \pi\ \pi\ 0$$

$$\text{Output}: \quad \underbrace{0\ 0\ \pi}_{G\ \text{Mode}}\ \underbrace{\pi\ 0\ 0\ \pi}_{U\ \text{Mode}}.$$

Error

Note that the regenerator responds to sames and changes, not to absolute phases.

Therefore, the comparator must be designed to detect transitions between modes of operation and to respond to these transitions.

The comparator is identical in design and construction to the dif-

ferential phase detector except that both inputs to the first Riblet coupler are used. It is shown in Fig. 8. Let $S_n(t)$ and $R_n(t)$ represent the regenerated and reference signals in the nth time slot, respectively. Then

$$S_n(t) = S_0(t) \exp [j(\omega t + \alpha_n)]$$

and

$$R_n(t) = S_0(t) \exp [j(\omega t + \beta_n + \theta)],$$

where α_n and β_n are the phases of the nth pulse in the regenerated and reference signals respectively and θ represents the phase shift in the long delay line (which is introduced into the reference signal path in order that corresponding time slots of the reference and regenerated signals be compared) and the phase shifter in the reference signal path. A straightforward analysis of Fig. 8 shows that the output of the comparator in the kth time slot is

$$V_k = \tfrac{1}{2}[\cos(\beta_k - \beta_{k-1} - \varphi) - \cos(\alpha_k - \alpha_{k-1} - \varphi) + \sin(\beta_k - \alpha_{k-1} + \theta - \varphi) + \sin(\alpha_k - \beta_{k-1} - \theta - \varphi)].$$

From this equation one can see the following results for the cases of interest. First $V(\varphi = 0, \theta) = -V(\varphi = \pi, \theta)$ for all values of θ.

Consider the case $\theta = 0$, $\varphi = 0$. There is a pulse of amplitude ± 1 whenever an error is made and no pulse when there is no error. The pulse is positive if the regenerated signal changes phase and the reference signal does not. It is negative if the reference signal changes phase and the regenerated signal does not.

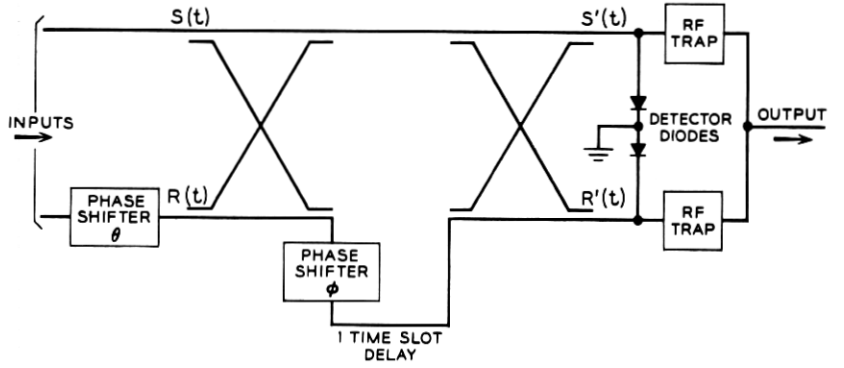

Fig. 8 — Comparator for AM-DCPSK repeater.

Consider the case $\theta = \pi/2$, $\varphi = 0$. There is a pulse of amplitude ± 2 whenever the regenerated signal changes from the G to the U mode but no pulse when the signal changes from U to G. ($\theta = -\pi/2$ gives a pulse on a U $\rightarrow$ G transition but not G $\rightarrow$ U.) The sign of the pulses is as described in the $\theta = 0$ case. This type of operation gives exactly a scale-of-two reduction in the counting rate and an increase of 6 dB in pulse height of the error signal. Since both of these effects are beneficial, this type of operation was generally used.

3.1.5 *Error Counting Circuit*

The detected output of the comparator contains cancelled pulses except where an error has occurred. Errors results in additions of the compared pulses which appear as either positive or negative output pulses. Since only pulses of one polarity can be counted at a time, the positive pulses are eliminated and only the negative pulses counted. Two settings of the comparator phase shifter, φ, 180 degrees apart, are therefore required to make a complete count of the errors.

The output signal is fed into a tunnel-diode unipolar amplitude discriminator (See Fig. 9). This is another Goto-pair of the type used in the regenerator but it is center-biased negatively to prevent positive input pulses from switching a diode. No timing is used. When a negative pulse of sufficient amplitude is received, the pre-biased diode switches to its second state and remains there for a maximum of 2 nsec, at which time the reflected pulse from a short-circuited delay line quickly returns it to its first state and it is ready to receive another pulse well before the next time slot.

The input level is adjusted so that only error pulses are passed. This is to prevent counting as errors the half-amplitude pulses which result from an occasional absence of pulses in time slots of the input signal, These are not properly to be considered as errors but only as trivial deductions from the 160-Mb/s total.

The output from the tunnel-diode amplitude discriminator is fed into a pulse amplifier followed by another amplitude discriminator and thence into a Hewlett-Packard 524-C Counter.

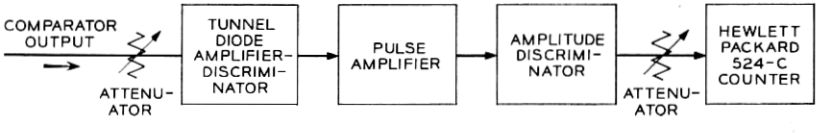

Fig. 9 — Error-counting circuit.

3.2 *Procedure*

3.2.1 *Adjustment of the Random Signal*

The statistics of the signal can be adjusted by changing the level and/or spectrum of the noise which drives the random word generator as well as by adjusting the bias on the various stages of the random word generator. Necessary conditions for a random signal, which were verified by monitoring both the envelope and the differentially detected "random" signals on the sampling scope are

(*i*) the number of pulses in the two phase states be equal,
(*ii*) the number of changes equal the number of sames, and
(*iii*) the four possible transitions (same → same, change → change, same → change, change → same) between time slots be equally populated.

The signal was made to satisfy these three requirements. They constitute our only check on randomness.

3.2.2 *Calibration of Noise and Signal Power*

The average noise power was read directly on a Hewlett-Packard Model 431B power meter. This calibration was checked frequently during the course of the experiment and was held to ±0.1 dB.

The noise came primarily from a noise source consisting of two model M1917 travelling-wave tubes in tandem followed by a 280 MHz filter. (An additional −26.5 dBm of noise was introduced by TWT 1).

The peak signal power was determined by detecting the envelope of the signal with a calibrated detector and setting the level for a peak power of +12.0 dBm. This measurement depends on the calibration of the detector diode, ability to read the pulse height as displayed on the sampling scope accurately, and the choice of which pulse height to use, since intersymbol interference caused several pulse heights to be present. The experimental error here is estimated to be ±0.4 dB.

Once the peak signal power, S, is set at +12.0 dBm, the average signal power corresponding to S, $\langle S \rangle$, can be read on the power meter. The value of $\langle S \rangle$ can be reproduced with an accuracy of ±0.1 dB and other values of pulse power can be set by changing $\langle S \rangle$ the appropriate amount. Thus even though the absolute value of S is in question by ±0.4 dB, the error in the *relative* power levels for the same pulse shape is only ±0.2 dB.

3.2.3 *Determination of Threshold*

Consider a situation where the peak signal power, S, going into the differential phase detector is sufficient for proper operation of the regenerator and the noise power is negligible. Now if S is slowly decreased, a value S_1 will be reached where some errors occur. As S is further decreased, a second value S_2 (about 2.5 dB below S_1) is reached where the regenerator begins to completely disregard the input signal. We define the threshold, T, as

$$T = \tfrac{1}{2}(S_1 + S_2).$$

One finds experimentally that $T \approx 0$ dBm.

3.2.4 *Determination of Intersymbol Interference*

In the presence of intersymbol interference, the envelope-detected pulse will have several values at the decision point due to the four possible states of its nearest neighbors. The ratios of these pulse heights (in dB) can be measured directly on a sampling scope. From this the value of ρ_T, where

$$\rho_T = 20 \log \frac{S_0(0)}{S_0(T)}$$

with S_0 as defined in (1), can be calculated.

3.2.5 *Summary of Experimental Errors*

The experimental errors are summarized in Table II.

3.2.6 *Timing and Center Bias Adjustments*

The timing for the signal pulses and the regenerator is derived from a single 160-MHz clock. The decision time was set by adjusting the

TABLE II — SUMMARY OF EXPERIMENTAL ERRORS

Quantity	Experimental error (dB)
Peak signal power—absolute value	±0.4
Peak signal power—relative value	±0.2
Average noise power	±0.1
Threshold	±1.0
S/N (absolute)	±0.6
S/N (relative)	±0.3
S/T (absolute)	±1.2
S/T (relative)	±0.2
ρ_T	±1.5

timing of the regenerator pulse for minimum error count with a very small input signal.

The center bias setting of the first regenerator strongly influences the ratio of errors made in detecting changes, N_c, to errors made in detecting sames N_s. In the presence of time crosstalk, the optimum setting of the center bias is not zero but rather in the direction to favor changes. In the experiments performed with resolved pulses (no intersymbol interference) the center bias setting was determined by balancing N_c and N_s at a value of S/N such that $N_c + N_s \approx 80$ counts per second. In the experiments performed with unresolved pulses (significant intersymbol interference), the center bias setting was determined by finding the two values of center bias where, in the absence of signal and noise, the regenerator jumps from one state to the other and taking the midpoint between these values. This setting does *not* optimize (exactly) the error rate, but it does allow a more direct comparison with theory.

3.3 *Results and Comparison With Theory*

3.3.1 *Narrow-Pulse Experiment*

The first experiment to be discussed is the measurement of error-rate as a function of S/N for several values of S/T. For this experiment, the filter F_1 was removed entirely and filter F_2 was placed between the second noise tube TWT-N2 and the noise attenuator. The pulses were then completely resolved as seen in Fig. 10(a). The eye diagram (output of the differential phase detector) is shown in Fig. 10(b). The experimental results are plotted in Fig. 11 along with the corresponding theoretical curves.[6]

The theory for this comparison assumes that all pulses are of the same peak power S, whereas in fact the modulator produces pulses of two slightly different amplitudes. This is an important effect for small values of S/T and probably accounts for part of the discrepancy in the data for S/T = 4.5 dB and a great deal of the discrepancy for S/T = 3.0 dB. Also note that small errors in determination of threshold are extremely important when S/T $\approx$ 3.0 dB.

3.3.2 *Unresolved-Pulse Experiment*

Filters F_1 and F_2 (as shown in Fig. 2) were adjusted to have 6-dB bandwidths of 250 MHz and 262 MHz, respectively. The overall 6-dB bandwidth of the two filters in series as used in the experiment was then 173 MHz. This widened the pulse considerably. The pulse envelope

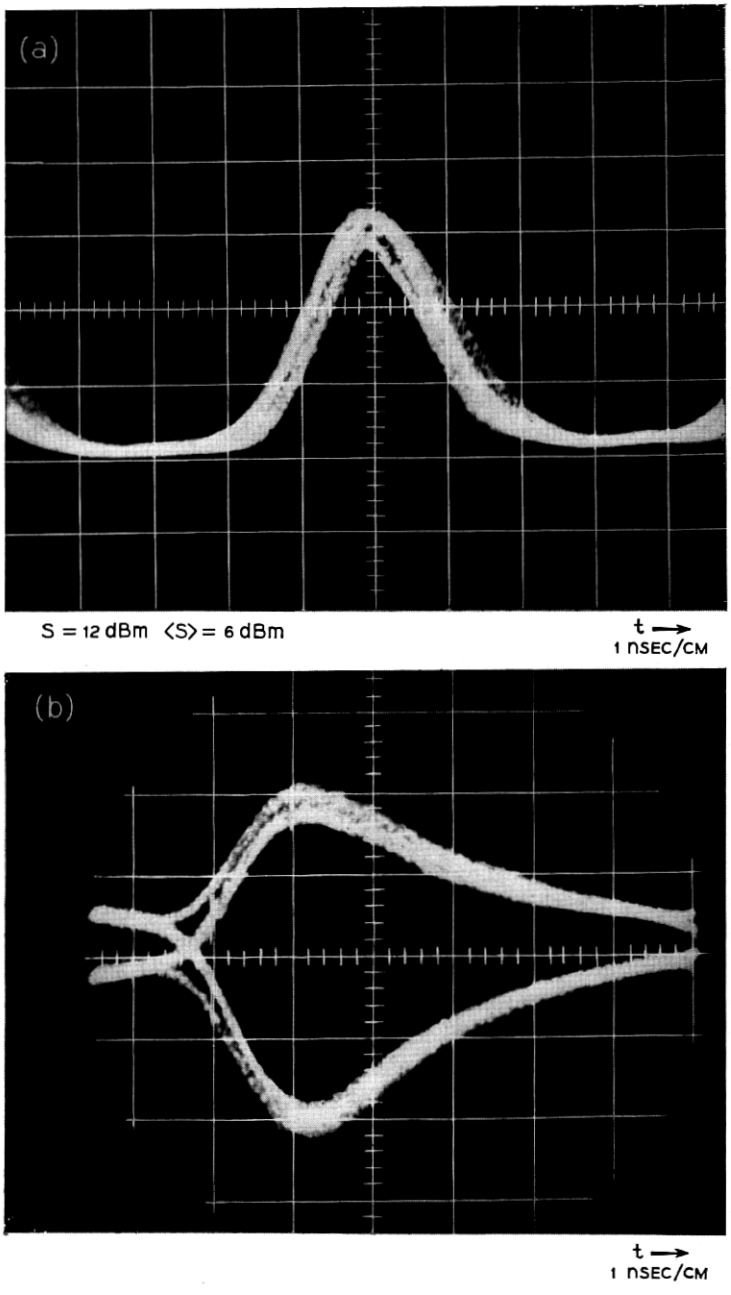

Fig. 10 — Narrow pulse experiment wave forms. (a) Envelope-detected RF pulse. (b) Eye-diagram (output to differential phase detector, input to regenerator).

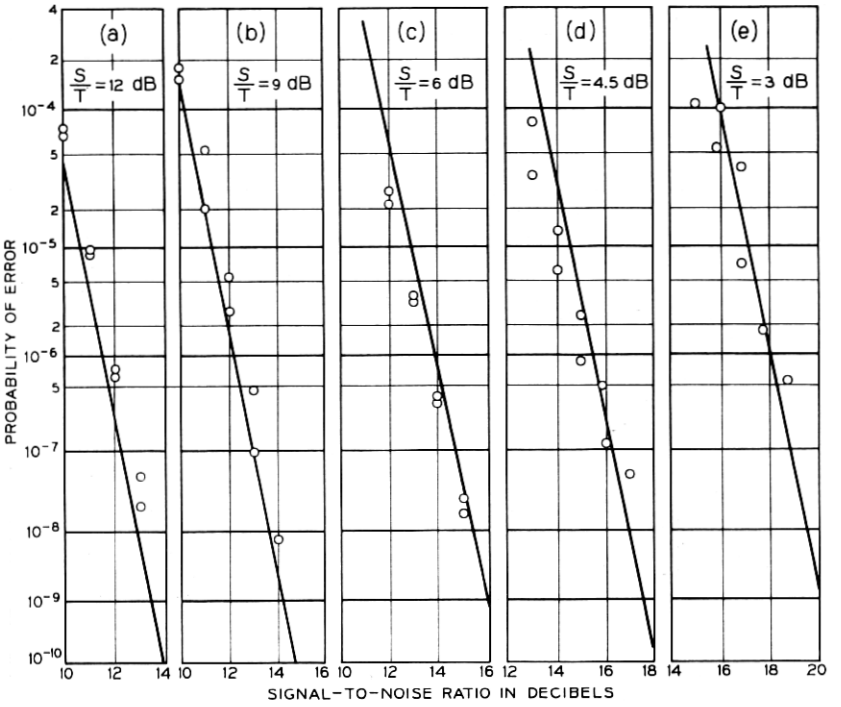

Fig. 11 — Error rate vs S/N for narrow pulses (negligible intersymbol interference). Points represent experimental values; curves are theoretical results from Ref. 6.

and the eye diagram for this signal are shown in Fig. 12. The intersymbol interference, ρ_T, was measured to be 22.5 ± 1.5 dB per tail. The experimental results are plotted in Fig. 13 along with the theoretical curves.

3.3.3 *Factor-of-Two Experiment*

Various arguments have been presented in the past which (erroneously) conclude that (at least under conditions of low error rate) an error in decision results in two errors (in adjacent time slots) in the regenerated signal. Salz and Saltzberg[7] have shown that these arguments are fallacious and that a single error in decision results, with about 90 percent probability, in a single error in the regenerated signal at the error rates used in these experiments.

Since these double errors, if they existed, would occur in adjacent time slots, our counter (video bandwidth is 10 MHz) would not be able

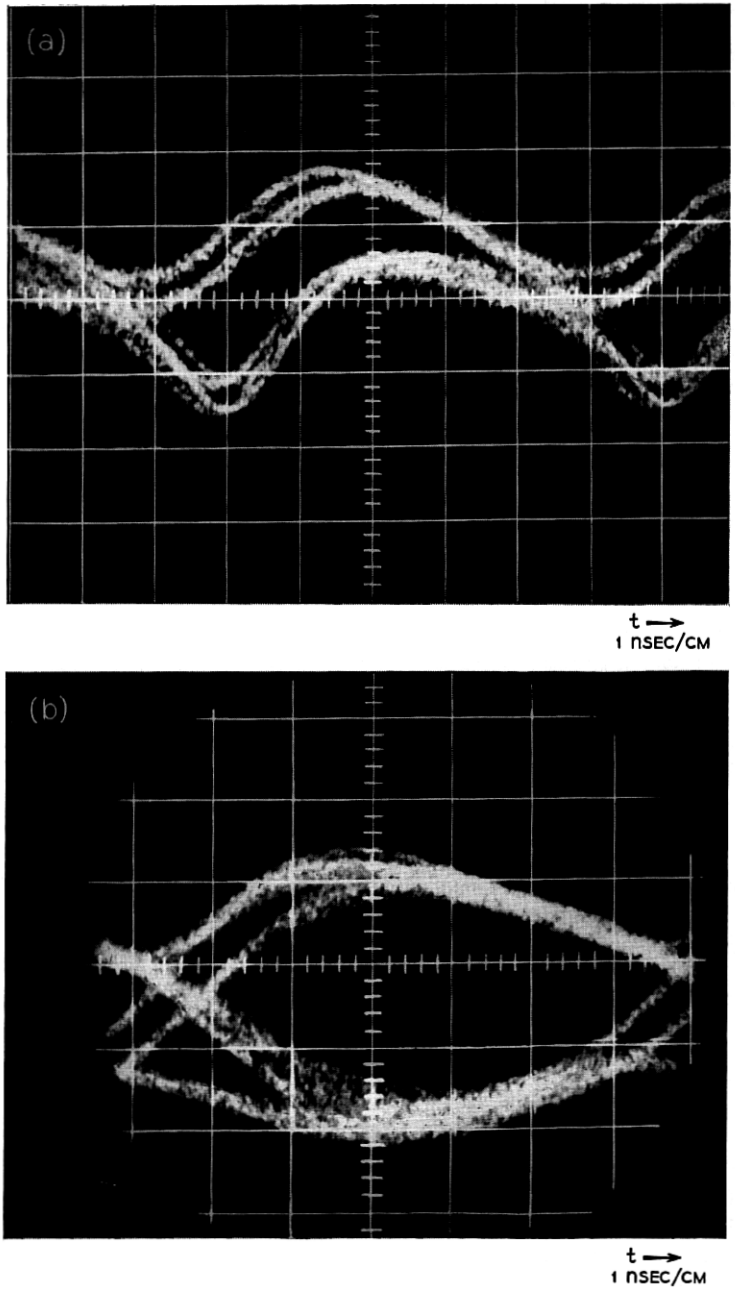

Fig. 12 — Widened pulse experiment wave forms. (a) Envelope-detected RF pulse. (b) Eye-diagram (output to differential phase detector, input to regenerator).

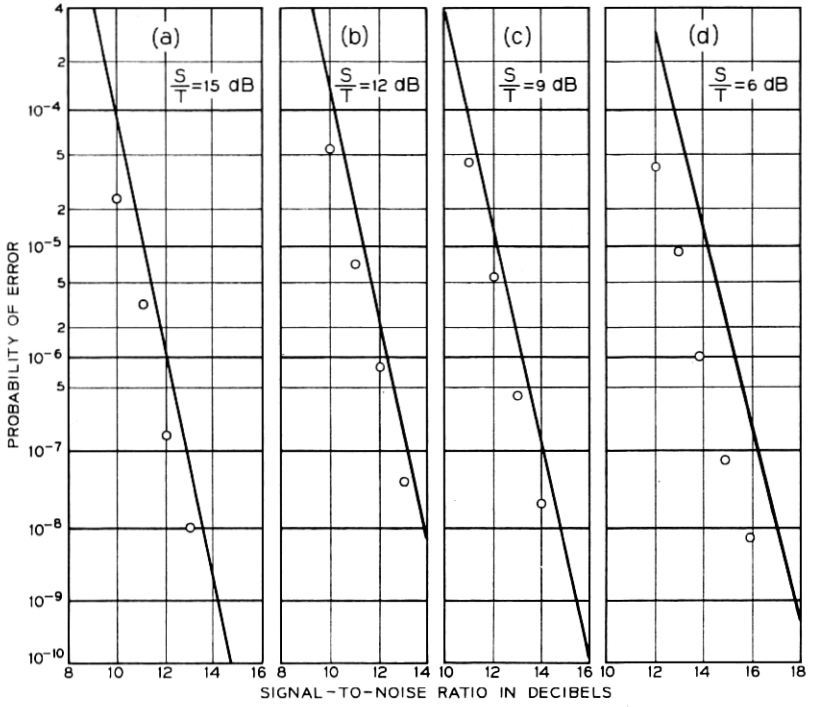

Fig. 13 — Error rate vs S/N for band-limited pulses. Points represent experimental values, curves are theoretical values from Ref. 5 evaluated $\rho_T = 22.5$ dB (the experimentally determined value for this waveform).

to resolve these pulses without benefit of the scale-of-two feature of the comparator. As explained in Paragraph 3.1.4 this scale-of-two can be removed by changing the phase of the reference signal 90 degrees. When this is done, the total count should double if the number of double errors is negligible. On the other hand, if double errors were created for every decision errors, the total count would increase only 50 percent since (for random signals) half of the "secondary" error-pulses from the comparator would be of the same polarity as their associated "primary" error pulses and hence could not be resolved in the counter.

Within experimental errors of a few percent, the total count is doubled when the scale-of-two is removed indicating that the errors in the regenerated signal do *not* occur in pairs.

3.3.4 *Test of Effect of Phase Error in the Differential Phase Detector on Error Rate*

The degradation in S/N produced by a small error, $\delta\varphi$, in the phase shift (or equivalently in the length) of the delay loop of the differential phase detector has been calculated.[5] This effect is of interest because $\delta\varphi$ is a function of temperature; hence, it cannot be made and kept arbitrarily small in a practical repeater. Fig. 14 shows the experimental points and the theoretical curve of equivalent degradation in S/N as a function of $|\ \delta\varphi\ |$. The points designated ○ were taken with $\delta\varphi < 0$, those designated □ with $\delta\varphi > 0$.

IV. THE FM-DCPSK REPEATER

4.1 *General Description of the FM-DCPSK Repeater*

Fig. 3 is a block diagram of the FM-DCPSK repeater. The overall operation of this repeater is quite similar to that of the AM-DCPSK repeater described in the preceding section. The random word generator, error counting circuit, and RF noise source are identical to those described in Paragraphs 2.1, 3.1.5, and 2.1, respectively.

4.1.1 *FM Deviator*

The pulse modulator used in the AM repeater is replaced with an FM deviator. This FM deviator consists of a frequency-modulated Esaki

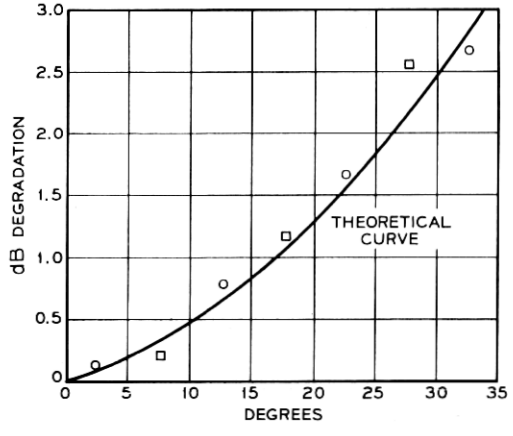

Fig. 14 — Degradation in effective S/N as a function of phase shift error in the differential phase detector.

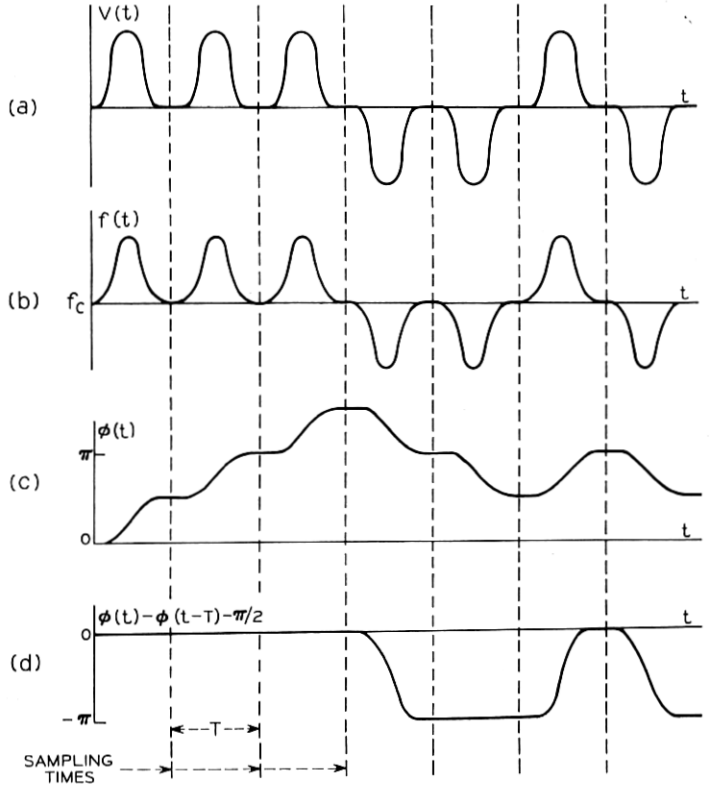

Fig. 15 — FM-DCPSK signal; (a) modulating voltage vs time; (b) frequency vs time; (c) phase vs time; (d) differential phase vs time.

diode oscillator. Modulation is produced by pulsing the bias voltage either positively or negatively in every time slot. The binary information is contained in the choice of polarity. This voltage pulse causes the oscillator frequency f to deviate from its nominal value f_c. This is illustrated in Fig. 15(a) and (b). This modulation causes a phase change $\delta\varphi_n$ given by

$$\delta\varphi_n = \int_{nT}^{(n+1)T} \{f(t) - f_c\}\, dt.$$

During the nth time slot sampling is performed after the phase shift has been completed (i.e, at the center of the intervals on which $f(t)$ equals f_c in Fig. 15(b); thus, $\delta\varphi_n$ represents the phase change between the nth and the $(n+1)$th samples.

Optimum noise immunity is obtained when the two possible signal states are anticorrelated, that is, when the two possible values of $\delta\varphi_n$ differ by π. This is achieved by adjusting the pulse amplitude until $\delta\varphi_n$ equals $\pm\pi/2$. In the following it will be assumed that this condition is satisfied.

The phase (relative to the phase of the carrier frequency) $\varphi(t)$ for the modulation illustrated in Fig. 15(a) and (b) is shown in 15(c). The differential phase detector used for this type of modulation is identical to the one described in the Paragraph 3.1.1. The phase shifter is adjusted to add (or subtract) a constant $\pi/2$ shift in the delayed signal so that it compares $\varphi(t)$ with $\varphi(t - T) + \pi/2$. Since $\varphi(t)$ and $\varphi(t - T)$ differ $\pm\pi/2$, $\varphi(t)$ and $\varphi(t - T) + \pi/2$ differ by 0 and π and the decision making circuitry operates just as it did for the system described in Section III. The quantity $\varphi(t) - [\varphi(t - T) + \pi/2]$ is illustrated in Fig. 15(d).

The requirements on the FM deviator differ from the usual requirements on an FM modulator in that only the area under the frequency-versus-time curve is important. There is no requirement that frequency be a linear or even a continuous function of the voltage.

Each of the FM deviators built for this experiment consists of a 0.5-mA GaAs Esaki diode mounted directly across 50-mil high X-band waveguide with one terminal grounded and the other brought out through an 11.2-GHz coaxial trap[8] as shown in Fig. 16. They have an output power of the order of −17 dBm. They are quite stable and have suffered no noticeable degradation over periods of up to 6 months.

The effect of the modulation on the amplitude of the output of the FM deviator turns out to be very small if the oscillator is properly tuned. Even after filtering the output to the bit-rate-bandwidth the amplitude variation is only about ±1 dB. Since the $\pm\pi/2$ modulation gives complete symmetry about the carrier frequency f_c, the optimum value of the free-running frequency of the PLO driven by this signal is also f_c.

4.1.2 *Baseband Regenerator*

The baseband regenerator used in this repeater is just the first stage or "first regenerator" of the device used in the AM repeater. Instead of driving a state switcher this "first regenerator" drives the FM deviator directly. The function of the state switcher, namely, to translate from straight binary to differential binary is accomplished automatically by the manner in which the FM deviator functions.

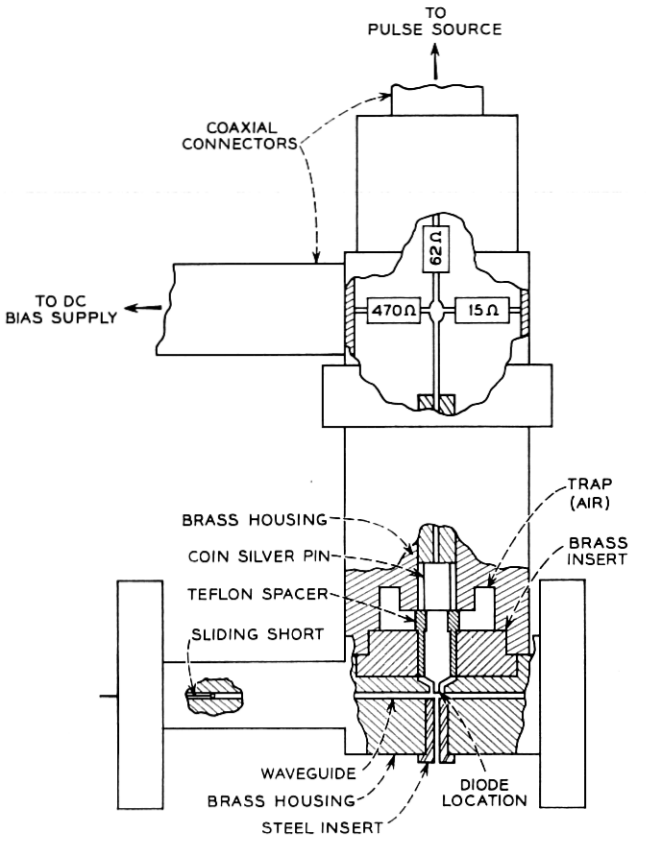

Fig. 16 — FM deviator.

4.1.3 *Timing Recovery*

One of the problems associated with any digital regenerative repeater is that of providing a clock to allow proper sampling of the received signal. The type of signal used in this experiment is particularly suitable for timing recovery because there is a frequency change in each time slot regardless of the message statistics. In this repeater, the timing was recovered by taking a portion of the incoming signal and putting it into a device which is like the differential phase detector except that the delay line is approximately 0.6 bit interval long. This device is described in the appendix.

4.1.4 *Limiter*

An Esaki diode limiter was incorporated into the circuit in order to take advantage of the improvements predicted in Ref. 6. This device consisted of an Esaki diode oscillator built directly in 50-mil high X-band waveguide. Input and output was accomplished by means of a Riblet coupler in the experimental repeater (only because a circulator was not at hand). In addition to limiting, the device gave about 20 dB of gain.

The repeater was operated both with and without the limiter; results of both types of operation are given in Paragraph 4.3.

4.1.5 *Comparator*

The comparison of input and output signals is made at baseband in this experiment (rather than at X-band as in the AM-DCPSK experiment). The output of the random word generator is split with a 6-dB matched splitter. One branch goes to the FM deviator, the other through a delay line to a baseband hybrid where it is compared with the output of the baseband regenerator. The polarities are such that if no error has been made the pulses cancel in the output arm of the hybrid whereas if an error has been made, the pulses add. This signal is then applied to the error counting circuit described in Paragraph 3.1.5.

Note that the baseband signal contains the information directly, not in differential form as does the X-band signal. Thus, some of the complicated logic of the X-band comparator is avoided.

4.2 *Procedure*

The procedure followed was similar to that described in Paragraph 3.2. The two significant differences are (*i*) the timing was derived from the timing recovery circuit, not from the 160-Mb/s clock which ran the random word generator, and (*ii*) the signal-to-noise ratio, when the limiter was used, was measured at the input to the limiter.

4.3 *Results and Comparison with Theory*

The results of experiments to measure error-rate versus S/N for the FM-DCPSK system are given in Fig. 17 for the case where a limiter was *not* used and in Fig. 18 for the case where a limiter was used. These results indicate that for an error rate of 10^{-9} the system operates with about 1.5-dB degradation from theoretical ideal without the limited and with about 0.5 to 0.8-dB degradation with the limiter. This

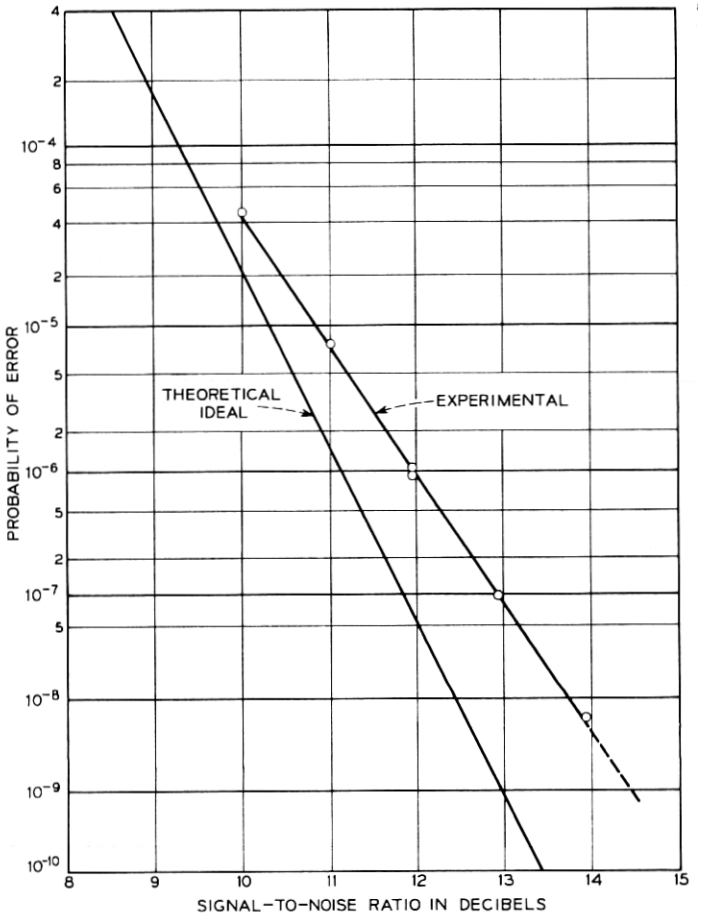

Fig. 17 — Error rate vs S/N for the unlimited FM-DCPSK signal.

degradation is due in part to the finite-width decision threshold discussed in Ref. 6 and in part to the intersymbol interference discussed in Ref. 5. The signal-to-threshold ratio is of the order of 12 dB for these experiments which, ignoring intersymbol interference, should account for about 0.4 dB of the degradation for the unlimited case. For the limited case the degradation due to a 12-dB signal-to-threshold ratio is about 0.1 dB. It is impossible to consider the intersymbol interference quantitatively because the exact form of the signal is unknown. Nevertheless, it is not unreasonable to assume that it

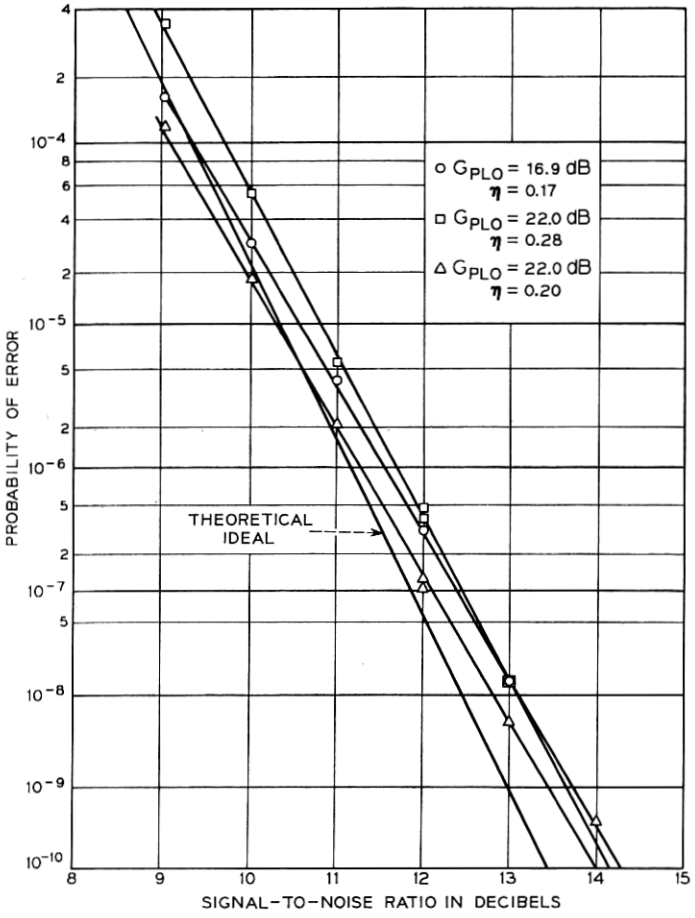

Fig. 18 — Error rate vs S/N for the limited FM-DCPSK signal.

accounts for a large part of the remaining discrepancy between the experimental and theoretical curves in Figs. 17 and 18.

V. CONCLUSIONS

Both AM-DCPSK and FM-DCPSK type systems are technically feasible. The FM-DCPSK type seems preferable in that timing information can be obtained by the method discussed above, whereas when the AM-DCPSK system is band limited to bandwidth of the order of the bit rate the pulses are no longer resolved and timing is quite

difficult to recover. In addition, a phase-locked oscillator serves as a suitable limiter for FM-DCPSK systems whereas a different—and perhaps more complicated—limiter would be necessary for the AM-DCPSK system. Finally, the baseband circuitry is much simpler for FM-DCPSK because the translation from straight binary to differential binary is accomplished automatically by inherent properties of the FM deviator.

VI. ACKNOWLEDGMENTS

The authors are particularly grateful to W. D. Warters for numerous suggestions throughout the course of these experiments, to H. M. James for assistance in construction of the X-band circuitry, and to J. H. Johnson for providing the X-band diodes for the limiters and the FM deviators.

APPENDIX

Timing Recovery from an FM-DCPSK Signal

The basic device described in the appendix of Ref. 5 and shown in Fig. 5 can be used as an FM discriminator for timing recovery by proper choice of the delay time τ. For this device one chooses τ such that $\omega_0\tau = m\pi$. Then (22) of Ref. 5 is, to first order, independent of the sign of $\omega(t')$ and thus independent of message statistics. One has

$$V(t) = \cos\left\{\int_{t-\tau}^{t} \omega(t')\, dt'\right\}. \tag{4}$$

The analysis cannot be carried further without assuming a particular form for $\omega(t')$. As an example, consider the signal given by (3) with $\omega(t')$ given by

$$\omega(t') = a_n \frac{\pi}{T} \cos^2 \frac{\pi t'}{T},$$

where $a_n = \pm 1$ depending on the message and changes sign only at the points $t' = (n + \frac{1}{2})T$. Substituting this into (4) gives

$$V_0(t) = \cos\left\{\frac{\pi\tau}{2T} + \tfrac{1}{2}\sin\left(\frac{\pi\tau}{T}\right)\cos\left(\frac{2\pi t}{T} - \frac{\pi\tau}{T}\right)\right\} \tag{5}$$

$$V_1(t) = \cos\left\{\frac{\pi}{T}\left[t - (n+\tfrac{1}{2})T - \frac{\tau}{2}\right] + \tfrac{1}{2}\cos\left(\frac{\pi\tau}{T}\right)\sin\left(\frac{2\pi t}{T} - \frac{\pi\tau}{T}\right)\right\}, \tag{6}$$

where (5) applies if a_n does *not* change sign on the interval $(t, t\text{-}\tau)$ and (6) applies if it does.

A study of (5) and 6) reveals that for $\tau \ll T$ the bit-rate-frequency component of V_0 and V_1 is quite small. As τ is increased, the bit-rate-frequency component of V_0 increases up to $\tau \approx 0.6T$ and then decreases to zero as τ is increased to T. The bit-rate-frequency component of V_1 increases as τ increases from zero to T. Thus, the optimum value of delay for the timing recovery discriminator is $\tau \approx 0.6T$.

The delay, τ, is related to T by another constant. Since we must have $\omega_0 T = (m + \frac{1}{2})\pi$ (see Appendix A of Ref. 5), and we also require $\omega_0 \tau = m'\pi$ for (4), τ and T are related by

$$\frac{\tau}{T} = \frac{m'}{m + \frac{1}{2}}.$$

Thus, one chooses m' such that $m'(m + \frac{1}{2})$ is as near 0.6 as possible.

REFERENCES

1. Miller, S. E., Waveguide as a Communication Medium, B.S.T.J., *33,* 1954, pp. 1209–1265.
2. Rowe, H. E. and Warters, W. D., Transmission in Multimode Waveguide with Random Imperfections, B.S.T.J., *41,* May, 1962, pp. 1031–70.
3. Kotel'nikow, V. A., *The Theory of Optimum Noise Immunity,* McGraw-Hill Book Co., New York 1959.
4. Lawton, J. G., Comparison of Binary Data Transmission Systems, Proc. Conf. Mil. Elec., 1958.
5. Hubbard, W. M., The Effect of Intersymbol Interference on Error Rate in Binary Differentially-Coherent Phase-Shift-Keyed Systems, B.S.T.J., this issue, pp. 1149–1172.
6. Hubbard, W. M., The Effect of a Finite-Width Decision Threshold on Binary Differentially Coherent PSK Systems, B.S.T.J., *45,* February, 1966, pp. 307–319.
7. Salz, J. and Saltzberg, B. R., IEEE Trans., *CS 12,* 1964, p. 202.
8. DeLoach, B. C., unpublished work.